Supporting Information:

Surface oxidation-induced restructuring of liquid Pd-Ga SCALMS model catalysts

Haiko Wittkämper[1+], Sven Maisel[2+], Michael Moritz[1], Mathias Grabau[1], Andreas Görling[2], Hans-Peter Steinrück[1], Christian Papp [1]

1: Friedrich-Alexander-Universität Erlangen-Nürnberg (FAU), Lehrstuhl für Physikalische Chemie II, Egerlandstr. 3, 91058 Erlangen, Germany

2: Friedrich-Alexander-Universität Erlangen-Nürnberg (FAU), Lehrstuhl für Theoretische Chemie, Egerlandstr. 3, 91058 Erlangen, Germany

+: shared first authorship

Fitting and quantitative XPS:

To discuss the intensity development in the Ga 3d, O 1s and Pd 3d regions during the *in situ* oxidation in form of reduced data (Figure 1d in the main publication), the signals needed to be deconvoluted into components assigned to the corresponding chemical species. The data processing was done using the software package Casa XPS 2.3.22. For the fitting of metallic Ga signals we used an asymmetric line shape, to be precise LF(0.6,1,70,300) as implemented in Casa XPS, the given parameters were optimized to reproduce the line shapes observed for a purely metallic liquid Ga samples. The line shape provides an asymmetry similar to that of a Doniach-Sunjic function while still having a finite integral (for details see Casa XPS manual). For the oxide shoulders observed for the Ga core levels we used Voigt-like line shapes, which we approximated using Gauss/Lorentz product functions (GL(30)) as implemented in Casa XPS. Similarly, the Pd 3d signal could be well reproduced using a symmetric Voigt-like line shapes (GL(40)). As discussed in the main text, alloying with Gallium is expected to result in a reduction of the asymmetry of the Pd 3d line shape. The O 1s signal that we observed was slightly asymmetric, likely due to additional contributions of sub stoichiometric oxides. To approximate the area of the O 1s signal we used a Gaussian/Lorentzian product formula modified by the exponential blend GL(60)T(1.8), this was found to reproduce the signal envelope well. An exemplary dataset is shown in Figure S1.

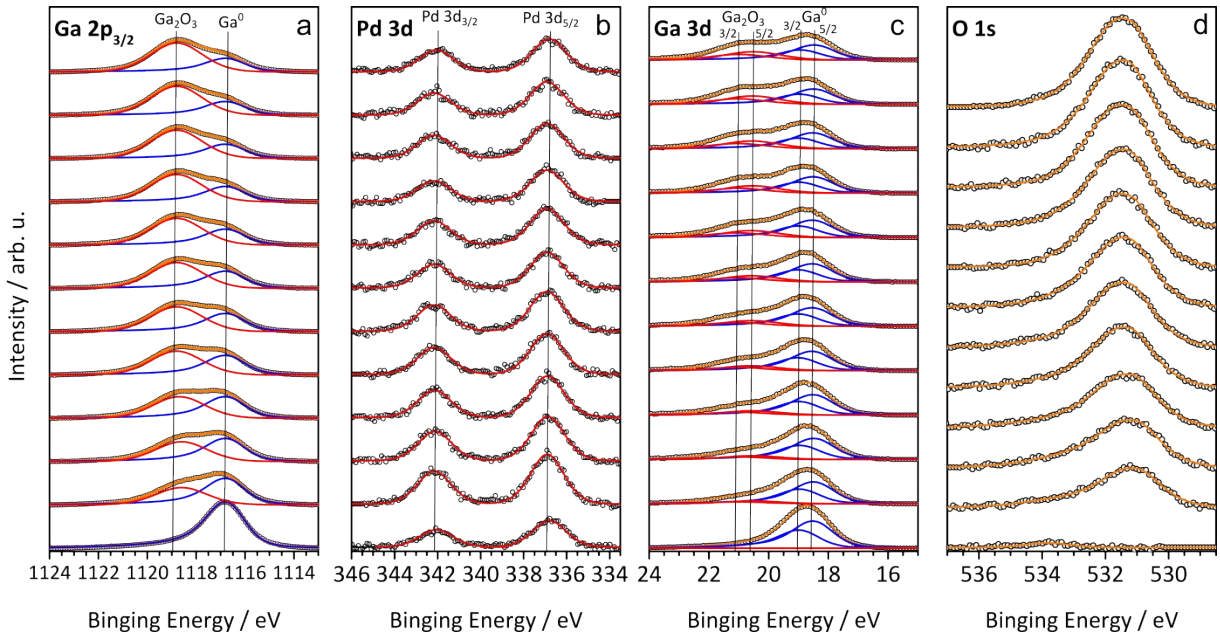

Figure S1: Dataset used for Figure 1 in the main Paper. Bottom spectra were collected in UHV prior to oxidation, the top most in UHV after oxidation and the spectra in between in-situ, during oxidation at 550 K and $3x10^{-3}$ mbar O_2. The final oxygen exposure totals $4x10^7$ L. a) shows the Ga $2p_{3/2}$ region with a metallic signal (blue) at 1116.7 eV and an oxidic signal (red) at 1118.7 eV;. b) shows the Pd 3d region with two spin-orbit split signals;. c) shows the Ga 3d region, that was deconvoluted using four signals: two spin orbit split doublets, one for the metallic components (blue) and one for the oxidic components (red); d) shows the O 1s region.

For quantifications we followed the same procedures as in our previous publications[1, 2]

The Ga_2O_3 film thickness was calculated from the ratio of the oxidized to the metallic component of the Ga 3d and Ga 2p signals according to:

$$D = \lambda_{i,Ga2O3}\, ln\left(\frac{I_{i,Ox}\lambda_{i,Ga}N_{Ga}}{I_{i,met}\lambda_{i,Ga2O3}N_{Ga2o3}} + 1\right)$$

Here, i denotes the core level (Ga 3d or Ga 2p), λ is the inelastic mean free path (IMFP)[3] in either gallium ($\lambda_{i,Ga}$) or gallium oxide ($\lambda_{i,Ga2O3}$) ($\lambda_{Ga\ 3d,Ga}$ = *30.9* Å, $\lambda_{Ga\ 2p,Ga}$ = 11.3 Å, $\lambda_{Ga\ 3d,Ga2O3}$ = 24.4 Å, $\lambda_{Ga\ 2p,Ga2O3}$ = 9.1 Å), and N_{Ga} and N_{Ga2O3} are the Ga densities in metallic Ga and in β-Ga_2O_3, respectively (N_{Ga} = 0.053, N_{Ga2O3} = 0.038, given in Ga Atoms per cubic Ångström).

The ratio between Ga and O was calculated using a simple model assuming no layering and just a homogeneous distribution of Ga and O:

$$\frac{[Ga]}{[O]} = \left(\frac{I_{Ga}}{\sigma_{Ga}T_{Ga}\lambda_{Ga}}\right):\left(\frac{I_O}{\sigma_O T_O \lambda_O}\right) \sim \frac{I_{Ga}}{I_O}$$

with I_{Ga} and I_O being the integrated areas of the gallium components assigned to gallium oxide and the O 1s signal. T is the analyzer transmission function, that was assumed to be the inverse kinetic energy of the photelectron E_{kin}^{-1}, σ are the photoemission cross sections ($\sigma_{Ga\,3d}$=0.01496, $\sigma_{Ga\,2p}$ = 0.4412, $\sigma_{O\,1s}$=0.04005)[4] and λ is again the inelastic mean free path of the photoelectrons in Ga_2O_3 ($\lambda_{O\,1s,Ga2O}$ = 18.38 Å, values for Ga are given above). The ratio I_{Ga}/I_O remains approximately constant during the experiments, see Figure S2 (a) and (b). Therefore, we conclude that there are no significant changes in the oxide film stoichiometry during our experiments. Deviation from the linear behavior, especially in Figure S2a, can be explained by the difference in kinetic energy of the O 1s and Ga 2p and thereby different attenuation by the gas phase.

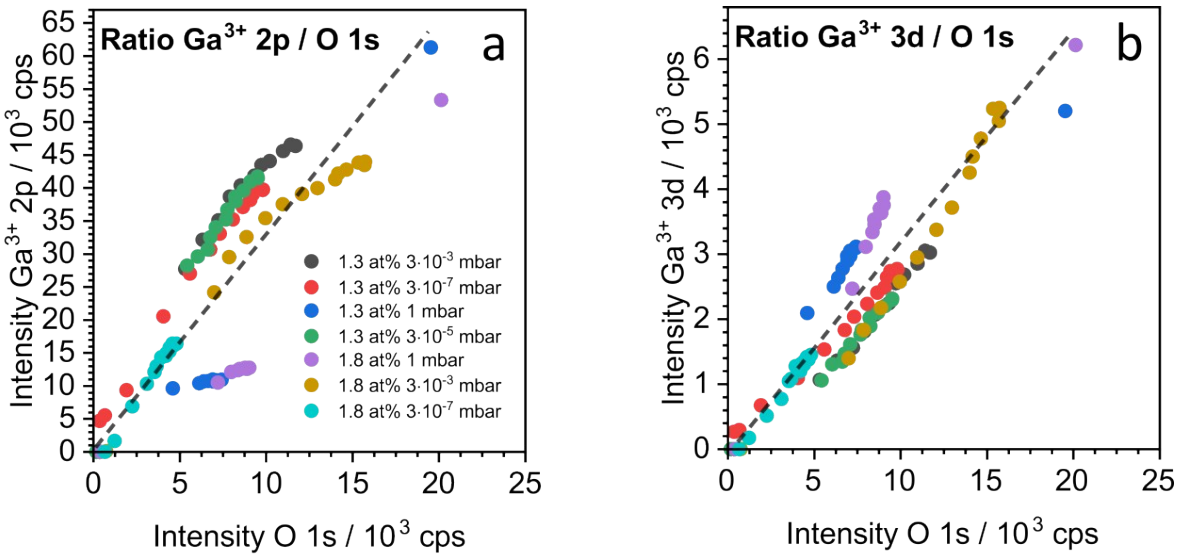

Figure S2: Ratio between the Ga^{3+} 2p and Ga^{3+} 3d intensities against the measured O 1s intensities during the in situ oxidation in (a) and (b). Please note that all but the last data points shown in each graph were recorded *in situ* and are therefore affected by the scattering of the gas phase.

In Figure 3 in the main text, the Pd fraction is given in at.% derived from the quantitative analysis of the Pd 3d and Ga 3d signal intensities is given according to:

$$\frac{\frac{I_{Pd\,3d}}{\sigma_{Pd\,3d}T_{Pd\,3d}\lambda_{Pd\,3d}}}{\frac{I_{Pd\,3d}}{\sigma_{Pd\,3d}T_{Pd\,3d}\lambda_{Pd\,3d}}+\frac{I_{Ga\,3d}}{\sigma_{Ga\,3d}T_{Ga\,3d}\lambda_{Ga\,3d}}} * 100\ at.\%$$

With $\sigma_{Pd\ 3d}$ =0.2197 and $\lambda_{\mathrm{Pd\ 3d}}$ = 26.592 Å.

We investigated the oxidation behavior in long term measurements of 327 h at 10^{-5} mbar and 120 h at 1 mbar. Figures S3 a and c show the time development of the oxide film thickness and Figures S3 b and d the development of the metallic and oxidic parts of the Ga 3d signals. As can be seen the thickness increases over the whole time of the measurements.

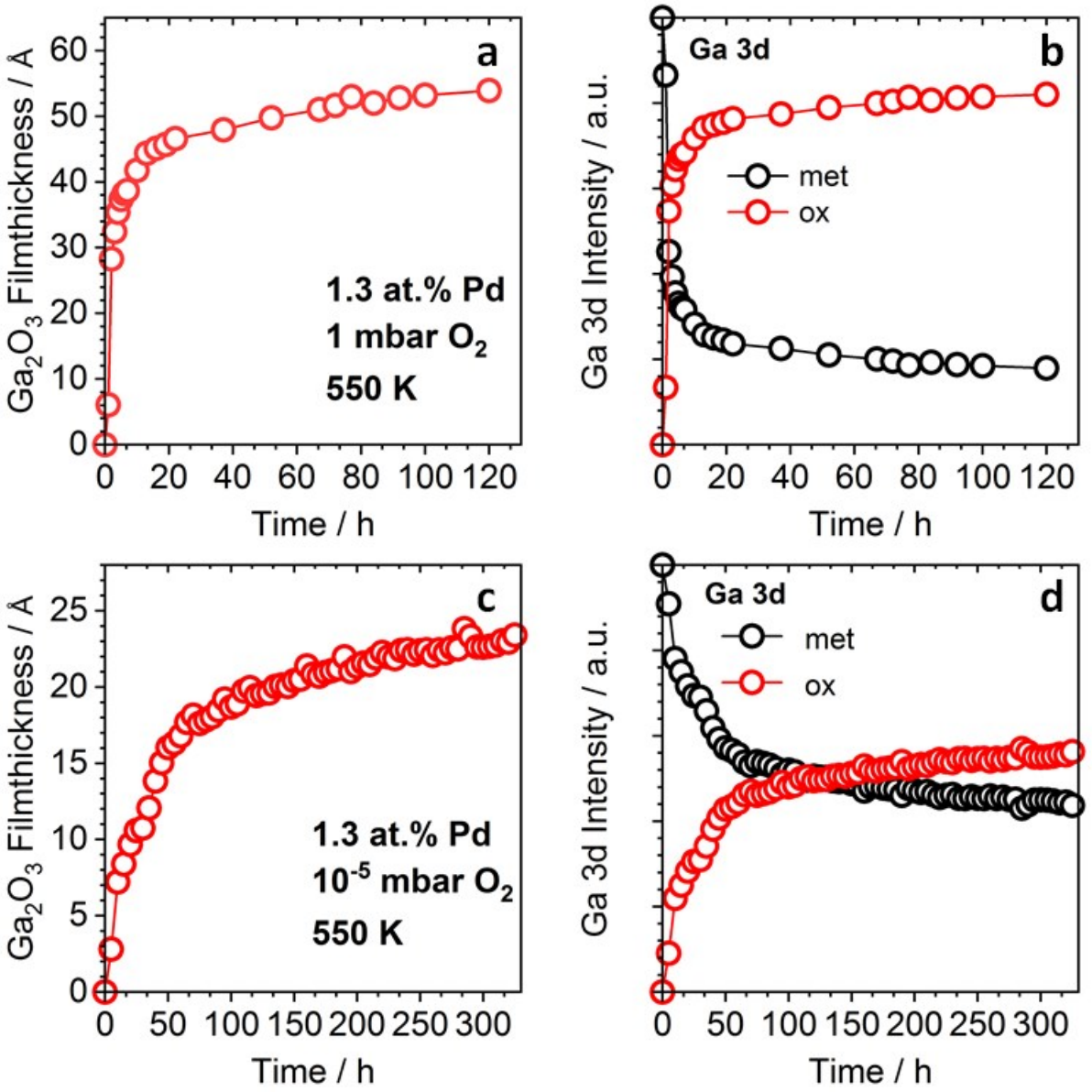

Figure S3: long term oxidation results for a 1.3 at.% Pd in Ga alloy at 1 mbar in a) and b) and at 10^{-5} mbar in c) and d).

DFT results:

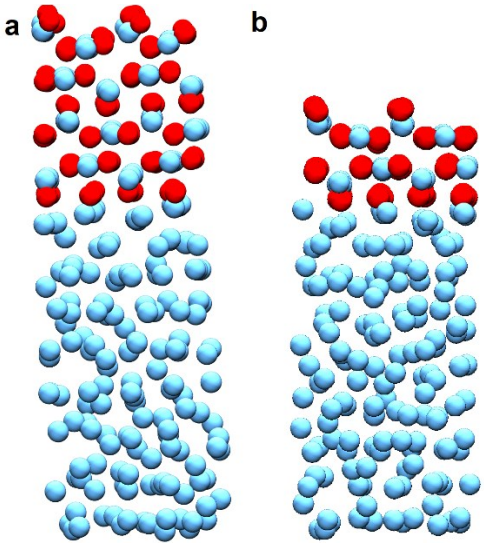

Figure S4: Comparison of the size of the slab models used in the geometry optimizations/core level calculations a) and the AIMD simulations b).

Interface structure:

Two different bonding patterns were observed in the AIMD simulations. This gets obvious by looking at the density profiles of Ga (Figure , main text and Figures S6b and S7b), which show a single peak for layer 1, i.e. the layer in direct contact with the last oxygen layer of the solid oxide, for simulations 1 and 3 (Figure and S7b) and a double peak in case of simulation 2 (Figure S6b). Cut-outs of the interface structures are depicted in Figure S5. This reveals that Ga can be bound in different ways, either coordinated to two O atoms of layer 0 (cf. Figure 6a) or bound to only one oxygen, thereby being located directly below a corresponding O atom. In simulation 2 where two peaks were observed in the density profile both types of bonding are equally present, i.e. 8 Ga atoms are bound to two oxygen atoms (first peak in density profile) and 8 Ga atoms are bound to only one O atom (second peak in the density profile). Altogether 16 Ga atoms per unit cell are present in this layer. The majority of the atoms remain in this interfacing layer for the whole simulation, showing that it is mostly static. On the other hand, simulations 1 and 3 display the case where only Ga atoms which are bound to two oxygen atoms are present, resulting in one Ga peak in the density distribution. The number of Ga atoms in this again mostly static layer is reduced to 12 atoms per unit cell. Below this mostly static interface layer, a strong layering is present for two more layers as shown in the density profiles, eventually decaying to a more homogeneous bulk like distribution in the layers underneath.

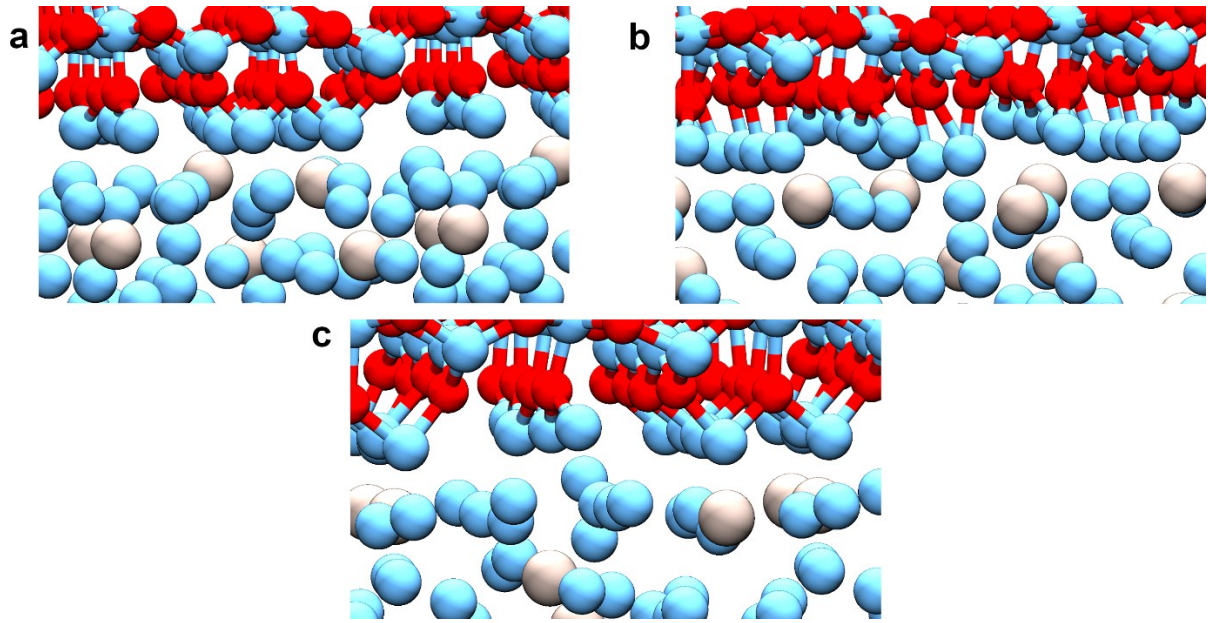

Figure S5: Cut-out of the interface using the final geometries of simulation a) 1, b) 2 and c) 3.

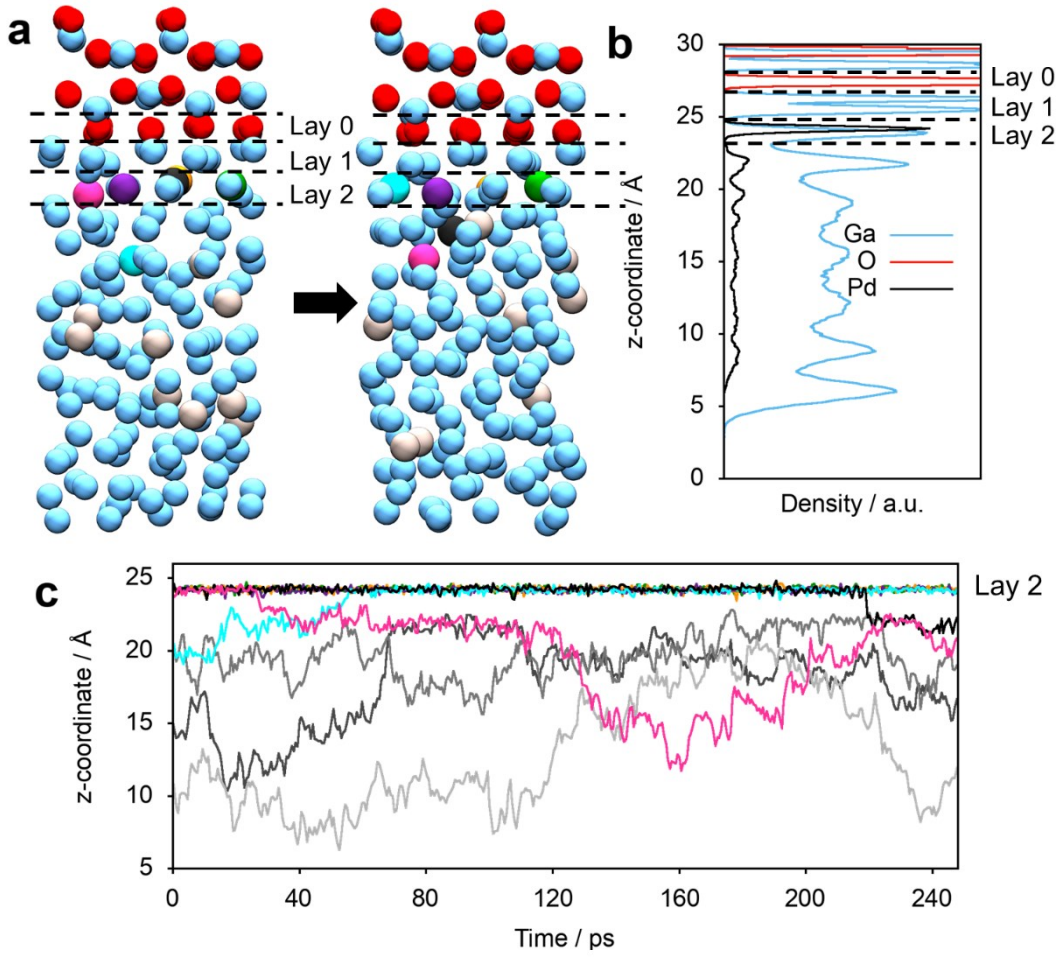

Figure S6: Results for simulation 2 analogous to Figure 5 in the main text for trajectory 1. Pd atoms which at some point in the simulation reach the interface (layer 2, cf. Figure 5) are

shown in different colors (a and c), Pd atoms which are not present at the interface in the simulation are shown in different shades of grey (c).

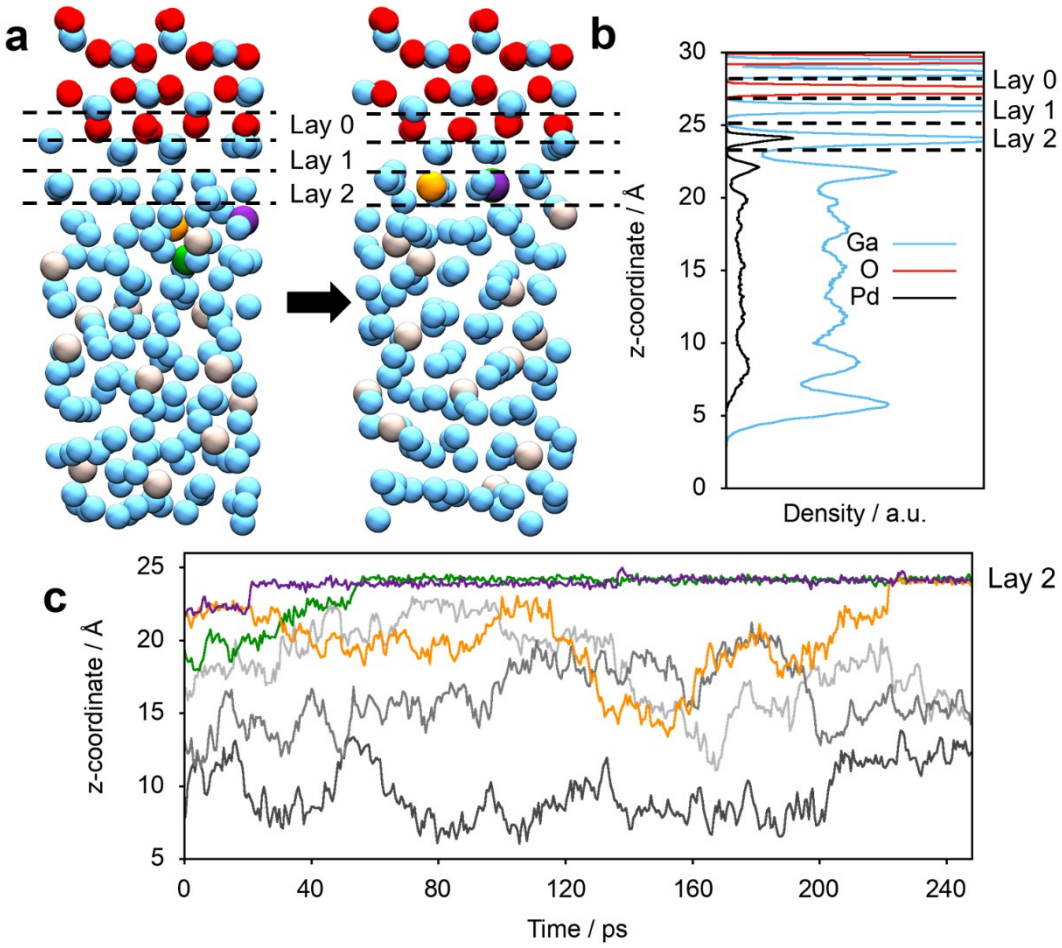

Figure S7: Results for simulation 3 analogous to Figure 5 in the main text for simulation 1. Pd atoms which at some point reach the interface (layer 2, cf. Figure 5) are shown in different colors (a and c), Pd atoms which are not present at the interface in the simulation are shown in different shades of grey in c).

Results of simulation 2 and 3:

Simulations 2 and 3 represent cases where the initial Pd concentration in layer 2 (cf. Figure 5a in the main text) is higher and lower, respectively, compared to simulation 1. The results are summarized in Figures S6 and S7. In simulation 2, five Pd atoms are present in layer 2 at the beginning of the simulation (shown in black, green, orange, purple and pink in Figure S6a and S6c). Only two of these Pd atoms (pink and black) leave the layer in the course of the simulation, while the other three remain in layer 2 the whole time. Additionally, one further Pd atom (cyan in Figure S6) diffuses to layer 2. The remaining Pd atoms (see Figure 6c, grey lines) are more mobile and diffuse through the liquid part of the slab. The described behaviour leads to a strong peak in the Pd density profile in the second layer (see Figure S6b).

In simulation 3 we start with an initial configuration where the interface is Pd depleted. However, it is observed in the simulation that three Pd atoms (orange, green and purple in Figure S7) arrive at the interface and stay there for extended simulation times. This leads to an increase in the Pd density in layer 2, see Figure S7b. In conclusion, these results show that independent of the starting configuration, that is the interfacial structure and the initial Pd concentration at the interface, an enrichment of Pd at the interface is observed in AIMD simulations, which strongly supports the experimental results.

Literature:

1. Grabau, M., et al., *Surface enrichment of Pt in Ga2O3 films grown on liquid Pt/Ga alloys.* Surface Science, 2016. **651**: p. 16-21.
2. Haiko Wittkämper, S.M., Mingjian Wu, Johannes Frisch, Regan G. Wilks, Mathias Grabau, Erdmann Spiecker, Marcus Bär, Andreas Görling, Hans-Peter Steinrück, Christian Papp, *Oxidation induced restructuring of Rh–GaSCALMS model catalyst systems.* The Journal of Chemical Physics, 2020. **153**(10).
3. Tanuma, S., C.J. Powell, and D.R. Penn, *Calculation of electron inelastic mean free paths (IMFPs) VII. Reliability of the TPP-2M IMFP predictive equation.* Surface and Interface Analysis, 2003. **35**(3): p. 268-275.
4. Yeh, J.J. and I. Lindau, *Atomic Subshell Photoionization Cross-Sections and Asymmetry Parameters - 1 Less-Than-or-Equal-to Z Less-Than-or-Equal-to 103.* Atomic Data and Nuclear Data Tables, 1985. **32**(1): p. 1-155.